ResearchGate

See discussions, stats, and author profiles for this publication at: https://www.researchgate.net/publication/264093854

Effect of Chain Structure on the Rheological Properties of Vinyl Acetate–Vinyl Alcohol Copolymers in Solution and Bulk

ARTICLE *in* MACROMOLECULES · JULY 2014

Impact Factor: 5.8 · DOI: 10.1021/ma5003326

CITATIONS
4

READS
40

10 AUTHORS, INCLUDING:

Alexander Malkin
Institute of Petrochemical Synthesis
312 PUBLICATIONS **2,774** CITATIONS
SEE PROFILE

Valery Kulichikhin
Institute of Petrochemical Synthesis
301 PUBLICATIONS **978** CITATIONS
SEE PROFILE

E. A. Litmanovich
Lomonosov Moscow State University
37 PUBLICATIONS **201** CITATIONS
SEE PROFILE

Yaroslav V Kudryavtsev
Russian Academy of Sciences
62 PUBLICATIONS **355** CITATIONS
SEE PROFILE

Available from: Alexander Malkin
Retrieved on: 02 February 2016

Macromolecules

Article

pubs.acs.org/Macromolecules

Effect of Chain Structure on the Rheological Properties of Vinyl Acetate–Vinyl Alcohol Copolymers in Solution and Bulk

Sergey O. Ilyin,[†] Alexander Ya. Malkin,[†] Valery G. Kulichikhin,[‡] Yulia I. Denisova,[†] Liya B. Krentsel,[†] Georgiy A. Shandryuk,[†] Arkadiy D. Litmanovich,[†] Ekaterina A. Litmanovich,[‡] Galina N. Bondarenko,[†] and Yaroslav V. Kudryavtsev[†,*]

[†]Topchiev Institute of Petrochemical Synthesis, Russian Academy of Sciences, Leninsky prosp. 29, 119991 Moscow, Russia

[‡]Chemistry Department, Moscow State University, Leninskie gory 1, build. 3, 119991 Moscow, Russia

Supporting Information

ABSTRACT: Bulk and solution studies revealed a strongly pronounced effect of chain structure on the rheological and relaxation behavior of well-characterized vinyl acetate–vinyl alcohol copolymers of similar composition and polymerization degree. The frequency–temperature superposition principle is fully applicable to the random copolymers, which demonstrate all expected relaxation states, whereas a divergence of the reduced dynamic moduli–frequency dependences is observed for the multiblock copolymers. In the latter case, the terminal zone is sensitive to the self-assembling of vinyl alcohol blocks into (depending on the copolymer composition) crystalline or amorphous microstructures. The monomer unit distribution particularly affects properties of the copolymer solutions in *N*,*N*-dimethylformamide (DMF). 5% solutions behave as simple viscoelastic liquids at 20 °C and show viscoplastic behavior at −20 °C, where more blocky chains are characterized by up to 4 orders of magnitude higher yield stress values. The multiblock copolymer solutions demonstrate a pronounced viscosity hysteresis in the heating–cooling cycle, being absent in the random copolymers. 10% solutions of multiblock copolymers are practically gelatinous even at room temperature. The observed effects are explained by examining the peculiarities of hydrogen bonding in vinyl acetate–vinyl alcohol copolymers using FTIR spectroscopy. The multiblock copolymers are characterized by stronger hydroxyl–hydroxyl H-bonds and greater fraction of interchain hydroxyl–acetyloxy H-bonds providing aggregation of chains and high viscosity of the corresponding samples, whereas the random copolymers more strongly interact with the residual solvent. Dynamic light scattering studies prove that the relaxation of concentration fluctuations is completely diffusive, being bimodal in the random copolymers and trimodal in the multiblock ones. The fast mode in the latter case demonstrates anomalous concentration behavior. In the dilute regime, up to very low concentrations, multiblock copolymer chains form stable aggregates, and this fact correlates with an unusual growth of the reduced viscosity in the corresponding rheological experiments.

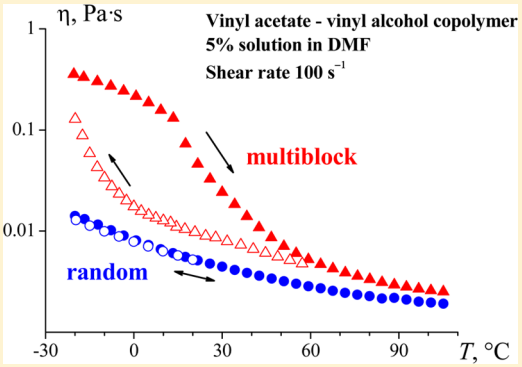

INTRODUCTION

Copolymers can be found among all types of polymers, ranging from biological objects, such as DNA, to numerous industrial polyolefins and synthetic rubbers. It is well-known that their chemical and physical properties depend not only on the nature of constituting monomers but also on their distribution along the backbone.[1] Regular block copolymers, especially di- and triblocks, are so far the most thoroughly studied objects,[2,3] as they can be synthesized with precise control of block lengths. The ability of such macromolecules to self-assemble into long-range ordered microstructures with the periodicity of 100–200 nm is systematically analyzed in theory and experiments and widely used in developing nanomaterials for lithography, membrane technology, transfer of light energy, data storage, and so on.[4−6]

Statistical copolymers are more common in chemical engineering due to the ease of their synthesis, though random structure of a polymer chain facilitates averaging rather than combining properties of two or more homopolymers in a single polymer material. Nevertheless, the ability of statistical copolymers to form complex (core–shell, vesicular, mushroom-like, etc.) structures in solutions upon temperature or pH variations, which can be enhanced by applying the concept of the conformation-dependent synthesis,[7] makes possible their use for drug delivery or molecular recognition in medicine and biology.[8−10]

Theoretical studies,[11−16] computer simulations,[17−26] and a few recent experiments[27,28] demonstrate that statistical (and even completely random) copolymers are capable of self-assembling in the melt state, too. Although microstructures with a long-range

Received: February 13, 2014
Revised: June 27, 2014
Published: July 11, 2014

 © 2014 American Chemical Society dx.doi.org/10.1021/ma5003326 | Macromolecules 2014, 47, 4790–4804

order can be formed at a very strong repulsion of comonomers only,[21,22] the conventional van der Waals interactions are predicted to cause compositional heterogeneities, which can noticeably affect the local mechanical properties[23−25] and crystallization behavior[26−28] of a sample. However, in practice statistical copolymers are mainly used in structural materials and a few examples related to the smart materials with shape memory,[29] conjugated oligomers for optoelectronics,[30] and polyelectrolyte-based fuel cells[6,31] only emphasize the advantages of regular block copolymers.

Meanwhile, there exists an intermediate situation, in which identical monomer units are grouped in blocks of variable length. In recent years studies of polydisperse di- and multiblock copolymers were started,[32−42] owing to the progress in controlled chain-growth polymerization.[43−45] It turned out that a disorder in the chain structure can be a positive factor that helps to control the parameters of various morphologies, for example, it enhances the stability of the bicontinuous gyroid phase[34,40] and increases the compatibilizing ability of copolymers.[42] One can expect that the potential of polydisperse copolymers will be revealed upon gaining more control over the chain statistics and, therefore, establishing different structure−property relations remains a relevant problem.

Polymer modification is another way to obtain polydisperse block copolymers.[46] For many reactions, it is possible to quantitatively describe the evolution of chain structure with time or conversion thus creating a basis for controlling various copolymer properties. In this paper, we consider a system of such kind. Our goal is to study how the difference in the comonomer unit distribution influences the rheological properties of vinyl acetate− (VAc−) vinyl alcohol (VA) copolymers in solutions and bulk and how the observed peculiarities are related to the interactions on a molecular level. Our choice of the model copolymer system, also known as "partially hydrolyzed poly(vinyl alcohol)", is not accidental. On a qualitative level, long ago it was known[47−50] that such properties of VAc−VA copolymers as the melting temperature, crystallinity, level of surface segregation, and degree of conversion in the iodine complex formation essentially depend on the macromolecular structure, which in turn is determined by the synthesis conditions.[51−55] VAc−VA copolymers form intra- and intermolecular hydrogen bonds. As was shown in ref 56, the alkaline hydrolysis (saponification) of poly(vinyl acetate) (PVAc) leads to multiblock copolymers with dominating hydroxyl−hydroxyl interactions, similar to pure poly(vinyl alcohol) (PVA).[57] At the same time, the reacetylation of PVA results in a random chain structure with competing hydroxyl−hydroxyl and hydroxyl−acetyloxy interactions, as the former type is more favorable energetically at room conditions but less thermally stable. Pronounced hydrogen bonding should also significantly affect the dynamic properties of VAc−VA copolymers and it is interesting to find correlations between those properties and the parameters of the comonomer unit distribution.

Recently[58] we demonstrated that the evolution of the chain structure with conversion in the course of PVAc saponification is well described by the neighbor effect model,[46] and we confirmed a nearly random comonomer unit distribution in the course of PVA reacetylation. With that notion, it is possible to use one master batch PVAc sample for synthesizing two series (multiblock and random) of VAc−VA copolymers that form pairs with close compositions and well-defined different chain structure. We began[59] a systematic comparison of their properties with studying crystallinity by the DSC-based method of thermal fractionation via successive self-nucleation and annealing.[60] The thickness of crystalline lamellas was related to the distribution of VA monomer units. In particular, it was shown that the minimum lamella thickness in all samples corresponds to a block of 15 VA units. Random VAc−VA copolymers containing 77 or less mol % of VA units are completely amorphous, while multiblock copolymers retain crystallinity even at the equimolar composition.

In the present paper, we continue the comparative study of multiblock and random VAc−VA copolymers of similar composition but different comonomer unit distribution with a focus on systematic measuring their rheological characteristics and establishing correlations with the data of DSC, FTIR spectroscopy, and static and dynamic light scattering on the physical structure of the copolymers. We will demonstrate, for the first time, that even a moderate tendency to block formation can cause drastic difference in the VAc−VA copolymers behavior in bulk and solutions.

While planning this research, we were encouraged by proved efficiency of rheological methods, especially in combination with optical and structural approaches, in studying characteristics of the microstructures formed by regular di-,[61] tri-,[62] and multiblock[63] copolymers and by associating polymers[64,65] in solution.

EXPERIMENTAL SECTION

Samples. Poly(vinyl acetate) (PVAc, Acros Organics, M_n = 4.8 × 10^4, M_w = 1.06 × 10^5) was reprecipitated from methanol into water. The precipitate was separated from the aqueous solution, dissolved in benzene, and purified by freeze-drying. The hydrodynamic radius of 7 nm in 3:1 (v/v) acetone−water mixture was measured by DLS at 20 °C.[58] Analysis of the ^{1}H NMR spectra showed that PVAc chains were atactic with the following microstructure (mol %): 25.8 iso-, 25.2 syndio-, and 49.0 heterotriads.

Poly(vinyl alcohol) (PVA) was obtained by quantitative saponification of PVAc carried out for 4 h at 30 °C in 3:1 (v/v) acetone−water mixture containing NaOH. The obtained sample did not contain residual VAc groups according to the ^{1}H NMR data. The average molecular masses M_n = 1.97 × 10^4, M_w = 3.86 × 10^4, and M_z = 6.04 × 10^4 determined by GPC in ref 59 correspond to the average degree of polymerization equal to ∼450 and the most probable (Flory) molecular mass distribution.

Multiblock VAc−VA copolymers were obtained by saponification of PVAc in the above-described conditions. The reaction was terminated at a desired conversion by adding 0.4 N HCl that neutralized the remaining alkali. The amount of HCl was calculated from the preliminary kinetic measurements carried out by back-titration. The obtained multiblock copolymer samples were denoted as MB15, MB26, MB52, and MB83, where the numbers correspond to the fraction of VAc monomer units in mol %.

Random VAc−VA copolymers were obtained by reacetylation of PVA prepared as described above. The reaction was conducted in acetic acid−water mixture at 100 °C until equilibrium was reached. The mixture composition was calculated following the lines of ref 47, which take into account that PVA is insoluble if the content of acetic acid is high. In order to avoid that difficulty, the copolymers containing more than 45 mol % of VAc units were obtained in two steps. The random copolymer samples were denoted as R13, R23, R50, and R70, where the numbers again correspond to the molar percentage of VAc monomer units.

All details of the syntheses can be found elsewhere.[58,59]

Solutions. Optically transparent solutions of PVA, PVAc, and VAc−VA copolymers in dimethyl sulfoxide (DMSO) and *N*,*N*-dimethylformamide (DMF) were prepared, except for MB15 and MB26 in DMF (form jellies up to 90 °C) and PVA in DMF (not soluble up to the DMF boiling point). The solutions of R50 and R70 copolymers were weakly brown-colored as a result of the long acid

dx.doi.org/10.1021/ma5003326 | Macromolecules 2014, 47, 4790−4804

Table 1. DSC and NMR Characteristics of PVAc, PVA, Multiblock, and Random VAc−VA Copolymers

			composition, mol %		triad fractions			average block lengths		
sample designation	T_g, °C	T_m, °C	VAc	VA	VAc−VAc−VAc	VAc−VAc−VA*	VA−VAc−VA	L_{VAc}	L_{VA}	randomness degree RD
PVAc	42	–	100	0	1	0	0	560	–	–
MB83	46	–	83.4	16.6	0.688	0.127	0.019	10	2.0	0.60
MB52	52	188	51.8	48.2	0.352	0.129	0.037	5.1	4.7	0.41
MB26	55	220	26.1	73.9	0.170	0.072	0.019	4.7	13	0.29
MB15	74	218	15.0	85.0	0.092	0.043	0.015	4.1	23	0.29
PVA	78	232	0	100	0	0	0	–	450	–
R13	73	143	12.6	87.4	0.006	0.042	0.078	1.3	8.8	0.90
R23	70	–	22.6	77.4	0.026	0.097	0.103	1.5	5.1	0.87
R50	63	–	50.0	50.0	0.168	0.255	0.078	2.4	2.4	0.82
R70	64	–	70.0	30.0	0.287	0.238	0.175	2.4	1.0	1.4

treatment that could lead to the formation of conjugated double bonds.[47]

The concentrations for the rheological studies were 1% and less, 5%, and 10% (wt/v) that corresponded to dilute, semidilute, and concentrated solutions, respectively. To intensify the dissolution process of MB52 and MB83 copolymers in DMF, the solutions were treated by microwave radiation of 450 W power during 30 s at 85 °C or just remained overnight in sealed ampules under Ar at 90 °C. It was checked by GPC that microwave heating did not affect the molecular mass distribution of the studied copolymers.

DLS studies demonstrated that the relaxation spectra of MB copolymers dissolved by fast microwave or long conventional heating were very similar.

Characterization. *Differential Scanning Calorimetry.* DSC measurements were carried out on a Mettler Toledo DSC823e calorimeter. The heating and cooling of samples was performed at a rate of 10 °C/min under argon flow (70 mL/min). The experimental data were treated using the STARe service program supplied with the device. The measurement accuracy was within ±0.3 °C for temperature and ±1 J/g for enthalpy. Glass transition and melting temperatures of the samples were recorded during the second heating run.

NMR Spectroscopy. The chain structure of VAc−VA copolymers was studied by ^{1}H NMR spectroscopy. The proton spectra for DMSO-d_6 solutions of the copolymer samples at 70 °C were recorded at a frequency of 600.22 MHz on a Bruker Avance 600 NMR spectrometer. The chemical shifts were determined with a precision of at least 0.001 ppm relative to the residual signal from DMSO-d_6 and recalculated relative to the shift of tetramethylsilane. The signals of different types of protons were attributed according to ref 66.

The copolymer composition (fraction of VAc units) was calculated as

$$P(\mathrm{VAc}) = \frac{I_{CH}(\mathrm{VAc})}{I_{CH}(\mathrm{VAc}) + I_{CH}(\mathrm{VA})}$$

where I_{CH}(VAc) and I_{CH}(VA) are the integral intensities of signals due to methine protons of VAc and VA-centered triads, respectively. The molar fractions of VAc-centered triads were determined from the integral intensities of signals due to VAcVAcVAc (4.82 ppm), VAcVAcVA* = VAcVAcVA + VAVAcVAc (4.95 ppm), and VAVAcVA (5.1 ppm). In the case of signal overlap, the deconvolution procedure in the 1D WINNMR program was used. The average lengths of VAc and VA blocks (L_{Ac} and L_A) and the randomness degree (RD) were calculated from the NMR data:

$$L_{Ac} = \frac{2P(\mathrm{VAc})}{R},\ L_A = \frac{2(1 - P(\mathrm{VAc}))}{R},$$

$$\mathrm{RD} = \frac{R}{2P(\mathrm{VAc})(1 - P(\mathrm{VAc}))}$$

where $R = P$(VAcVAcVA*) + 2P(VAVAcVA) is the so-called probability of a block boundary.[58]

Microstructure parameters of PVAc chains were evaluated from the ^{1}H NMR spectrum of a PVAc solution in $CDCl_3$ registered at 25 °C. Following ref 67, the intensities of methyl proton signals in syndio- (2.05 ppm), hetero (2.03 ppm), and isotactic (2.00 ppm) triads were used for that purpose.

A typical ^{1}NMR spectrum of VAc−VA copolymer (MB52) is shown in the Supporting Information, Figure S1a. Signals from all methylene (1.2−1.79 ppm) and methyl (1.95−1.97 ppm) protons in the dyads VAVA, VAVAc, and VAcVAc and triads VAcVAcVAc, VAcVAcVA* = VAcVAcVA + VAVAcVAc, and VAVAcVA are observed in the 1.2−2.2 ppm range. Signals at 2.50 and 3.12 ppm are attributed to DMSO-d_6 and H_2O, respectively. The 3.4−5.2 ppm range contains the signals of methine protons belonging to VA-centered triads (3.4−4.0 ppm) and VAc-centered triads (4.7−5.1 ppm). The latter range for MB52 and R50 copolymers is compared in Figure S1b.

The difference in VAc triad fractions, which is clearly seen at the NMR spectrum, is quantified in Table 1, being added with the calculated VAc and VA average block lengths and randomness degree for all the copolymers studied. As is expected, the tendency for block formation is revealed for all copolymers of MB series (their RD parameter is considerably less than unity), whereas R copolymers are close to completely random (Bernoullian) ones, for which $L_{VAc} = 1/P$(VA), $L_{VA} = 1/P$(VAc), and RD = 1. The only exception is R70 that exhibits a tendency to unit alteration, which could be related to a two-step procedure of its synthesis. In any case, this copolymer does not contain long blocks.

Glass transition and melting temperatures of the copolymers are also shown in Table 1. In the course of the hydrolysis T_g increases from 42 °C for pure PVAc to 78 °C for pure PVA, then it decreases during reacetylation, again with a peculiarity (unexpectedly high value) for R70. The copolymers with a high content of VA units exhibit an ability to crystallize, which is much more pronounced for the multiblock ones.

FTIR Spectroscopy. A solution of VAc−VA copolymer in DMF was poured onto a silicon optical glass plate (chip). After solvent evaporation and polymer film formation, the chip was placed into a Bruker high temperature controlled cell connected with Bruker IFS 66v/S FTIR spectrometer. Spectra were recorded in the transmission mode in the range of 400−4000 cm^{-1} (50 scans, resolution of 2 cm^{-1}) at room temperature and then at 50, 60, 80, 150, 180, and 210 °C after conditioning for 10 min at each point. Finally, heating was switched off and the spectra were recorded at cooling in the same regime until room temperature. For treating the experimental data, the software package Bruker OPUS−7 was used.

The analysis of interactions in VAc−VA copolymers was performed by comparing the IR spectra of MB52 and R50 copolymer films deposited from DMF solutions shown in the Supporting Information (see Figures S2−S4 and explanations therein). The main conclusions are as follows.

At room temperature MB52 copolymer is characterized by stronger H-bonds between OH groups entering VA monomer units that are capable of multiple self-association:[56,68]

dx.doi.org/10.1021/ma5003326 | Macromolecules 2014, 47, 4790−4804

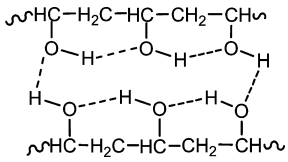

Upon heating above 60 °C, these hydrogen bonds begin to dissociate. At 210 °C the degree of association does not exceed 2−3 monomer units, yet isolated OH groups are absent and the difference between MB52 and R50 is still detectable, thus indicating that more stable H-bonded associates are present in the multiblock copolymer even after melting. Interestingly, at cooling of the samples in the absence of solvent no additional H-bonds between OH groups of VA units are formed. Such behavior could be related to low macromolecular mobility, which is insufficient to reach conformations that are favorable for the formation of new H-bonds.

At the same time, when MB52 is cooled down, a new band appears at 80 °C that becomes clearly distinguishable near room temperature. Most probably, there is a manifestation of copolymer crystallization, as is reported for pure PVA in the literature.[56]

The presence of residual DMF solvent in the copolymer films is detected. Already at room temperature the DMF content in R50 copolymer is much higher than in MB52, with the difference getting ever stronger at heating. From the FTIR data, DMF completely volatilizes from MB52 at 80 °C, while in R50 spectra the corresponding band disappears at 150 °C only. Variation in the absorption band position for R50 and MB52 films corroborates that the interaction of DMF with the random VAc−VA copolymer is stronger than with the multiblock one.

Broadening and shift of the bands corresponding to the carbonyl and ester stretching indicate that VAc units also take part in H-bonding including high temperature (>180 °C) region, when there is no traces of DMF in the both copolymers. Therefore, H-bonds are formed not only between two or more hydroxyl groups but also between an OH group of VA unit and an oxygen atom of VAc unit, in agreement with the literature data.[55,56] From our data, it is not possible to conclude, which of two oxygen atoms in acetyloxy group is preferentially involved into H-bonding and quantum chemistry calculations should be applied here. In any case, if VAc and VA units are chain neighbors, then they can form a hydrogen bond leading to a thermally stable 6- or 8-member ring.

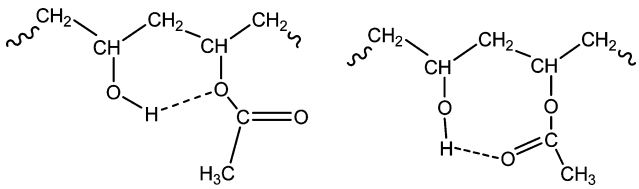

Since the average block length in R50 is ca. two monomer units, almost all VAc units are capable of intrachain H-bonding. In the case of MB52 copolymer, blocks contain in average five monomer units so that a substantial part of VAc units is flanked by other VAc units and therefore may interact with VA units only via formation of interchain H-bonds.

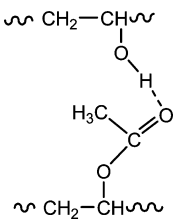

Thus, MB52 copolymer is characterized by stronger hydroxyl−hydroxyl H-bonds and more interchain hydroxyl-acetyloxy H-bonds than R50 copolymer. This conclusion underlies the difference in the bulk rheological behavior of those copolymers discussed below.

Rheology. Rheological properties of all samples were measured in the bulk at 40−220 °C and in the solutions in DMF and DMSO at −20 and +20 °C using an Anton Paar Physica MCR301 rotational rheometer. The temperature range for the melt was limited by its thermal oxidation.

The following series of measurements were carried out:

- dynamic modulus (storage and loss moduli, G' and G'') at a low-amplitude (linear) harmonic oscillation in the angular frequency range from 0.0628 to 628 s^{-1};
- viscosity (measuring shear stress) at a controlled shear rate of 10^{-4}−10^{2} s^{-1} by scanning for at least 30 s at every step;
- viscosity (measuring shear rate) at a controlled shear stress of 10^{-2}−10^{2} Pa by scanning for at least 180 s at every step;
- relaxation modulus in the linear viscoelasticity domain under step shear deformation;
- temperature dependence of the viscosity at the shear rate of 100 s^{-1} under the heating rate of 5 °C/min and cooling rate of 1 °C/min.

The parallel-plate geometry was used for measuring the dynamic modulus in the bulk and the cone−plate geometry was applied in all other cases.

It is worth mentioning that in the experiments with pure solvent at shear rates exceeding 10−100 s^{-1}, we observed secondary flows, which led to an apparent increase in the viscosity. However, the presence of a polymer in the solution suppressed this effect and shifted the onset of secondary flows to higher shear rate. For example, we found that adding only 0.1% of copolymer VAc−VA shifted the registered instability (observed as pseudodilatancy) from 160 to 600 s^{-1}.

Light Scattering. Prior to measurements, the solutions of VAc−VA copolymers in DMF were filtered through Millipore filters with hydrophilized Nylon membranes having the pore diameter of 0.45 μm.

A Photocor Complex laser light-scattering goniometer equipped with a HeNe laser (a wavelength of λ = 633 nm, an intensity of 25 mW) as a light source was used. The scattering angle θ was varied in the range 30−150°. In static (SLS) experiments, the total scattering intensity was measured. In dynamic (DLS) experiments, the time cross-correlation function g_2 of the scattered-light intensity fluctuations was determined with a 288-channel Photocor-FC correlator board and treated with the Alango DynaLS software through the inverse Laplace transform method to yield relaxation-time distributions.

RESULTS AND DISCUSSION

Bulk Rheology. Linear viscoelastic properties of VAc−VA copolymers were measured in a wide temperature range. The frequency domain at each temperature covered at least four decimal orders (see the Supporting Information, Figure S8). The difference between the behavior of random and multiblock copolymers becomes absolutely evident if the experimental data are analyzed with the aid of the frequency−temperature superposition principle.

Temperature of 120 °C was chosen as the reference temperature T_0 for constructing master curves for the random copolymers. Shift factor a_T was taken as the ratio of frequencies $\omega_0(T_0)$ and $\omega(T)$, for which the loss tangent, tan δ, is the same for the temperatures T_0 and T. However, the described approach did not work for the multiblock copolymers and we had to use the shift factors for MB15, MB26, and MB52 samples that were found for the corresponding random copolymers with close compositions. For MB83, the shift factor was calculated by matching the loss modulus. Temperature dependences of the shift factors are presented in Figure 1.

It is worth noting that the problem of constructing viscoelastic master curves for diblock copolymers, as well as for polymer blends, has a long history. It was proven that a general superposition in the wide temperature range based on a single temperature dependence of the shift factor is principally

dx.doi.org/10.1021/ma5003326 | Macromolecules 2014, 47, 4790−4804

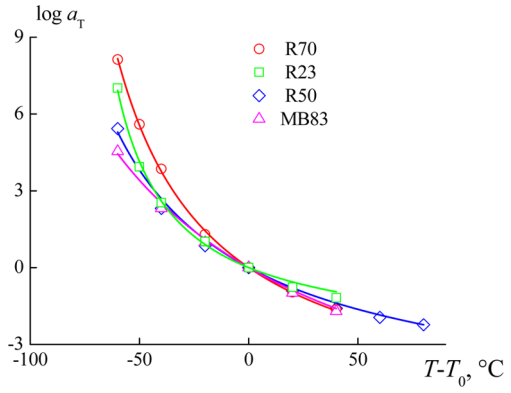

Figure 1. Temperature dependences of the shift factors a_T at the reference temperature T_0 = 120 °C.

impossible.[69] The reason for it is quite evident: the relaxation time for one block changes with temperature independently of that for another block. In ref 69, a rather laborious method for the summation of their contributions to the relaxation spectrum of the whole chain is proposed. It is unlikely that this approach can be applied to multiblock copolymers, because it is absolutely unclear how to summarize the relaxation characteristics of different blocks randomly distributed along a polymer chain.

The master curves obtained for R50 and MB52 copolymers by superposition based on the same temperature dependence of the shift factor are compared in Figure 2. One can see that the dynamic modulus behavior for R50 is quite traditional for amorphous polymers. In Figure 2a, the domains of flow (terminal zone) I, rubbery state II, transient state (vitrification) III, and glassy state IV are clearly observed. The most important fact is a good superposition of the data obtained at different temperatures. It means that the copolymer chains consisting of chemically different monomer units can be characterized by a unified temperature dependence of their relaxation properties.

Meanwhile, a quite different picture is seen for MB52 in Figure 2b, where the reduced data obtained at different temperatures do not superimpose in the low frequency range. Thus, an average VAc and VA block lengths of ca. 5 units (see Table 1) appear long enough to demonstrate the distinction of their relaxation properties. Also, it attracts attention that no terminal (flow) zone exists for MB52 copolymer in the studied frequency and temperature domains. Indeed, a decrease in the dynamic modulus can be found at low frequencies only at 220 °C. Such behavior can be explained by the formation of VA crystalline domains or intermolecular aggregates, in which VA and VAc units are connected with hydrogen bonds. This understanding is supported by the recent experiments with PE-based random copolymers[27,28] and corresponding Monte Carlo simulations,[26] which demonstrate that the self-organization of

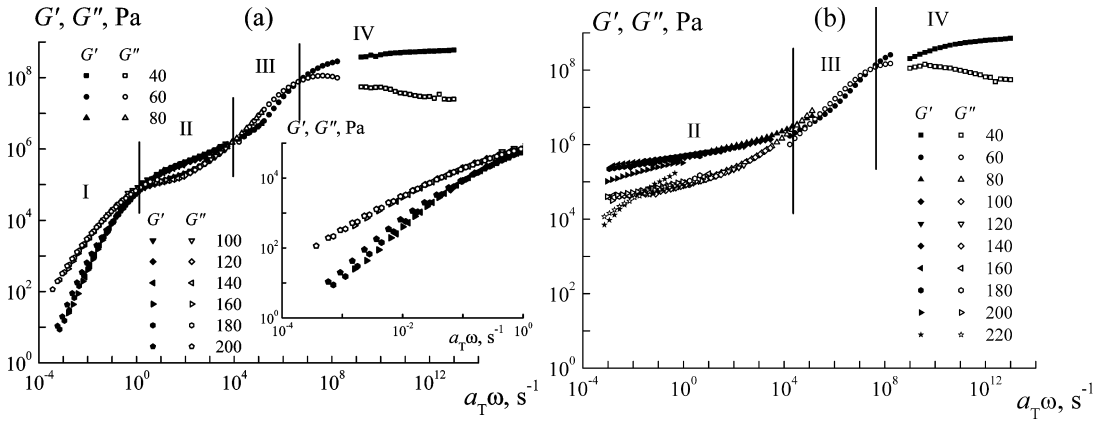

Figure 2. Frequency dependences of the storage (filled points) and loss (open points) moduli measured at different temperatures (shown) and reduced to 120 °C for (a) R50 and (b) MB52 copolymers. The inset gives a more detailed view of the low frequency domain.

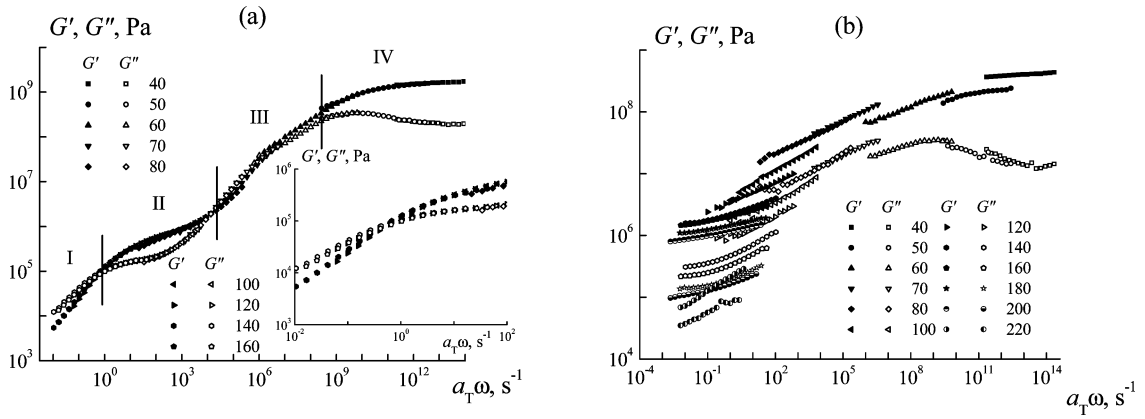

Figure 3. Frequency dependences of the storage (filled points) and loss (open points) moduli measured at different temperatures (shown) and reduced to 120 °C for (a) R23 and (b) MB26 copolymers. The inset gives a more detailed view of the low frequency domain.

dx.doi.org/10.1021/ma5003326 | *Macromolecules* 2014, 47, 4790−4804

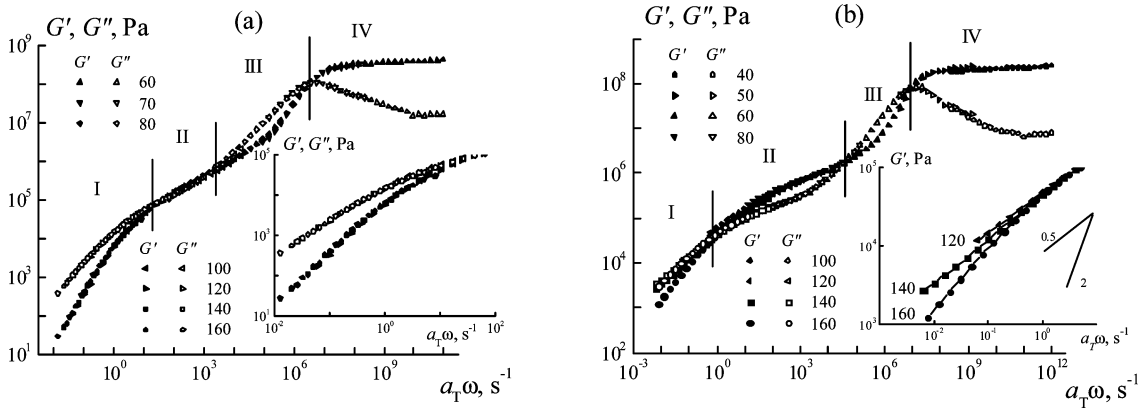

Figure 4. Frequency dependences of the storage (filled points) and loss (open points) moduli measured at different temperatures (shown) and reduced to 120 °C for (a) R70 and (b) MB83 copolymers. The insets give a more detailed view of the low frequency domain.

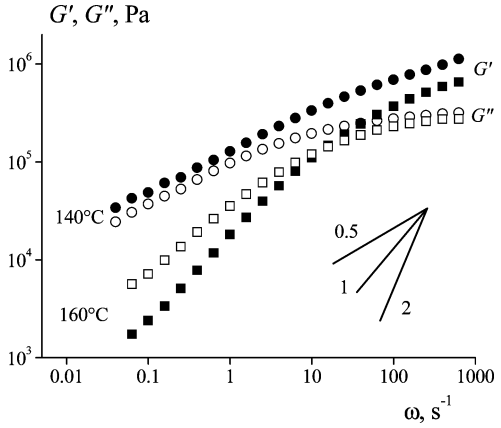

Figure 5. Frequency dependences of the storage (filled points) and loss (open points) moduli measured at two temperatures (shown) for R13 copolymer.

crystallizable blocks can take place at temperatures significantly higher than the melting point of such copolymers.

Rheological evidence of the structural transformations at low frequencies is corroborated by the DSC traces presented in the Supporting Information along with the temperature dependences of the dynamic modulus. As is seen from Figure S5, the glass transition for both copolymers takes place at a frequency of the order of 10^{-1} Hz. The DSC curve for R50 copolymer reveals a small endothermic peak near T_g, which presumably reflects the enthalpy relaxation due to physical aging of a sample during its storage in a glassy state.[70] The heat effect of melting for R50 is not detected (Figure S5a), whereas for MB52 a melting peak with the heat effect of ca. 13 J/g exists at 209 °C (Figure S5b). It corresponds to the degree of crystallinity for VA units of 17%, basing on the melting heat effect for PVA homopolymer reported in ref 71. Thus, the DSC data confirm the existence of ordering in MB52 in opposite to R50, being in agreement with the FTIR conclusion that the former copolymer is characterized by stronger H-bonds.

Increasing the content of VA units does not affect applicability of the temperature−frequency superposition to R23 random copolymer (Figure 3a) but leads to a much stronger divergence in the experimental data at attempted to construct the master curve for MB26 multiblock copolymer (Figure 3b).

Variations in the viscoelastic behavior clearly correlate with the fraction of crystallizable VA units. Whereas crystallinity is not detected in R23 (Figure S6a), as well as in R50 copolymer (Figure S5a), the DSC data directly indicate a substantial increase in the crystallinity of MB26 (Figure S6b) in comparison with that of MB52 copolymer (Figure S5b). The melting peak position shifts from 209 to 220 °C and the heat effect increases from 13 to 44 J/g, which corresponds to ca. 38% percent of VA units in the crystalline phase.

As was shown in ref 59, multiblock VAc−VA copolymers quantitatively obey the predictions of Flory's crystallization theory,[72] which relates the melting temperature (if it exists) to

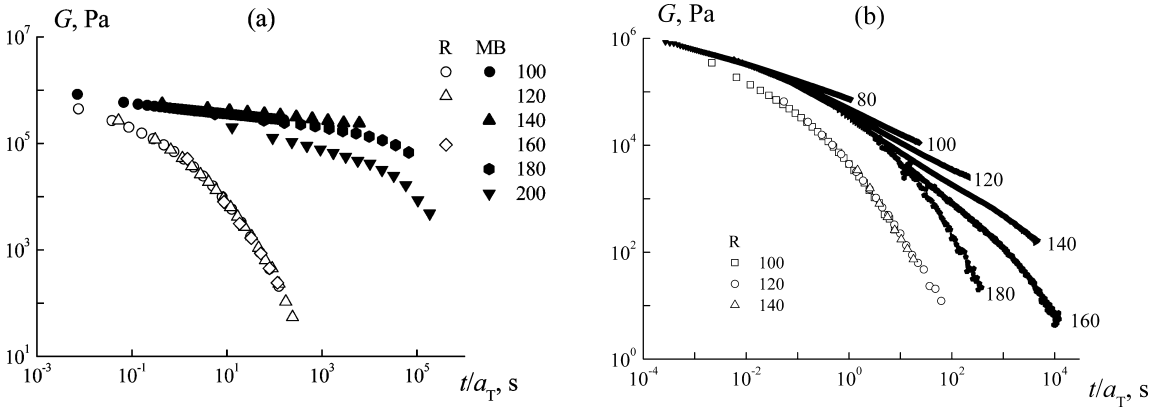

Figure 6. Time dependences of the relaxation modulus for the random (open points) and multiblock (filled points) copolymers. The data were measured at different temperatures (shown) and reduced to 120 °C for (a) R50 and MB52 and (b) R70 and MB83 copolymers.

dx.doi.org/10.1021/ma5003326 | Macromolecules 2014, 47, 4790−4804

the conditional probability to meet another VA unit next to a given one in the copolymer chain. At a fixed composition, such probability for a random copolymer is always less than that for a multiblock copolymer. This results in a much more steep decrease of T_m and the degree of crystallinity with increasing the fraction of noncrystallizable monomer units in the former case. It was shown that the crystallinity of random VAc–VA copolymers is reduced to zero at a much lower percentage of the VAc units so that all random copolymers studied in this work, except for R13, should be, and are, amorphous.

A quite different rheological picture is revealed in the copolymers with high content of VAc units. In that case, the terminal zone (flow domain) is present not only for R70 random copolymer (Figure 4a) but also for MB83 multiblock copolymer (Figure 4b).

Nevertheless, the superposition principle fails for MB83 copolymer in the low frequency domain, in opposite to R70 copolymer. Since the slope of the storage modulus dependence on frequency in log–log coordinates is equal to 0.5, as is seen from the inset in Figure 4b, microphase separation into a lamellar morphology can be assumed.[73,74] For years, the rheological evidence of a microstructure formation was reported for regular block copolymers only,[75] but recently it was found[27,28,76] that statistical olefin multiblock copolymers also can form long-range ordered mesostructures with a period several times larger than that in diblock copolymers of a comparable chain length. In this study, we observe the similar rheological behavior in the statistical multiblock copolymers of another type containing VA blocks that are too short to form crystalline lamellas but still able to self-assemble. The DSC data demonstrate the absence of melting for the both R70 (Figure S7a) and MB83 (Figure S7b) copolymers thus confirming that those samples are completely amorphous.

It is curious that a very similar behavior is demonstrated by R13 copolymer having nearly inverse composition. According to the DSC data, a very small crystallinity degree of 4% with T_m = 143 °C is characteristic for that copolymer. As is seen from Figure 5, both components of the dynamic modulus demonstrate the slope close to 0.5 at 140 °C and to 1 at 160 °C, thus indicating an order–disorder transition. It is not clear, whether the rheology can feel so subtle effect of crystallite melting or the transition is similar to what is observed for MB83 copolymer.

Thus, the experimental data obtained for the dynamic modulus in MB copolymers demonstrate that the frequency–temperature superposition principle fails even in the case of rather short VAc and VA blocks, which retain their individual relaxation properties. Similar conclusion can be done basing on the measurements of the relaxation modulus (Figure 6). Again, the superposition works well for all random copolymers but it is not applicable to MB copolymers with any percentage of VAc units. It is also worth noticing that in the latter case the relaxation is considerably slower, as it should be in more ordered systems.

Solution Rheology. *Intrinsic Viscosity.* In this study, we used the cone–plate rotational rheometry (instead of the standard capillary method) to avoid the shear rate effect in measuring the intrinsic viscosity. It is worth mentioning that using a modern high sensitivity rotational viscometer and a large surface plate makes it possible to reliably reach the shear stress of 0.003 Pa, which is much better than with any capillary viscometer in the range of low shear rates.

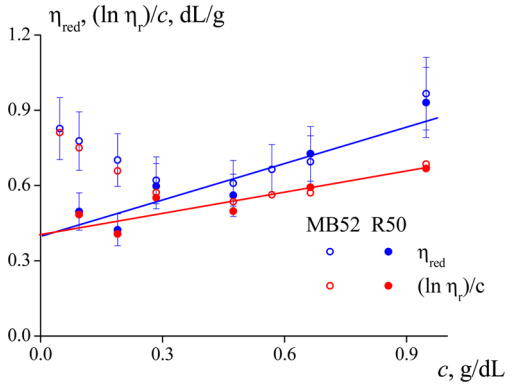

Figure 7. Concentration dependences of the reduced (blue) and inherent (red) viscosities for R50 (filled points) and MB52 (open points) copolymers in DMF at 20 °C. The solid lines fit the data for R50.

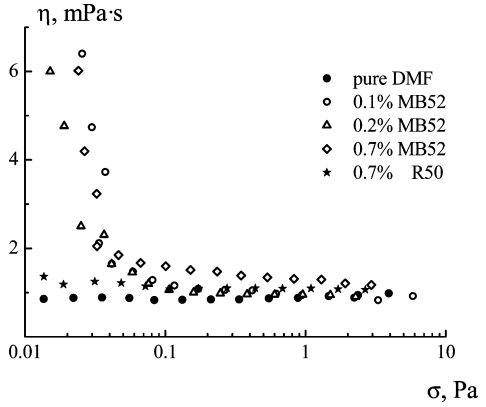

Figure 8. Flow curves for the dilute solutions of R50 and MB52 copolymers in DMF at 20 °C.

Our estimates show that the Reynolds number for standard capillary measurements with an ASTM Ubbelohde viscometer and DMF solvent is of the order of 1000, while in the rotational tests *Re* is of the order of 10. Thus, using a rotational viscometer allows us to carry out experiments at much lower shear rates (1–100 instead of 10^4–10^5 s^{-1}), which is important for the solutions under study. If one wants to reach shear rates of the same order using a capillary viscometer, then it is necessary to apply a unit with so high L/d ratio that the experiment would take several hours, which is clearly unreasonable.

That is why we have chosen the rotational rheometry and just this method has led to an unexpected result for the intrinsic viscosity of random and multiblock VAc–VA copolymers in DMF solution. As is seen from Figure 7, the dependence of the reduced viscosity on concentration for R50 copolymer can be fitted with a blue straight line (the Huggins law), with the intercept giving the intrinsic viscosity $[\eta]_{R50}$ = 0.39 dL/g. The same value can be obtained using the Kraemer fitting of the relative viscosity logarithm divided by the concentration (red line). The concentration dependence of the reduced viscosity for MB52 copolymer is also linear at c > 0.5 g/dL, but in decreasing concentration it goes through a minimum and begins to increase with dilution. Statistical analysis along the lines of ref 77 confirms that this result is not an experimental error. Thus, it is rather uncertain to indicate a certain value of the intrinsic viscosity for MB52 copolymer, which is at least as high as 0.9 dL/g.

dx.doi.org/10.1021/ma5003326 | *Macromolecules* 2014, 47, 4790–4804

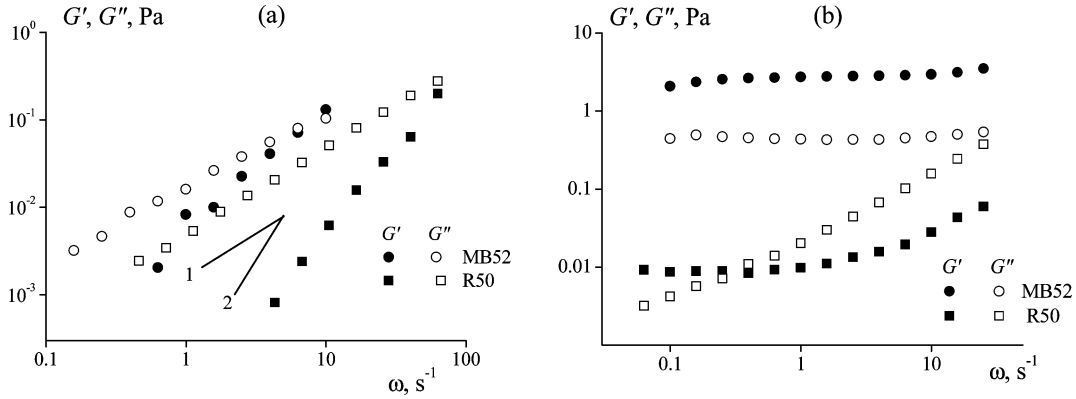

Figure 9. Frequency dependences of the storage (filled points) and loss (open points) moduli for (a) 5% and (b) 10% solutions of R50 and MB52 VAc–VA copolymers in DMF at 20 °C.

A viscosity anomaly at low concentrations of polymer solutions is known in capillary viscometry since Staudinger's times[78] and, being a subtle effect, got various explanations basing either on polymer adsorption on the capillary walls or on polymer–solvent interactions (see ref 79 for a comprehensive review). However, such effects are usually reported for concentrations below 0.1 g/dL, while we observe an upward deviation in the reduced viscosity at ca. 0.5 g/dL. Moreover, our measurements were performed on a rotational viscometer with a flow characterized by considerably lower (about 2 orders of magnitude) Reynolds numbers than flows in a typical (Ubbelohde) capillary viscometer. Therefore, we believe that the observed anomaly is due to aggregation of macromolecules caused by interchain interactions. Similar rheological behavior was recently reported for dilute polyacrylonitrile solutions in DMSO[80] and supramolecular aqueous L-cystein/Ag-based gels.[81] In the both cases, presence of the long sequences of identical units is an essential condition, which is apparently fulfilled in our study for the multiblock but not for the random VAc–VA copolymers.

Aggregation of MB52 copolymer chains in the dilute solutions in DMF results in the appearance of the yield stress. From the flow curves plotted in Figure 8 we find $\sigma_Y \approx 0.05$–0.07 Pa, which is close to the accuracy limit of the viscometer. Though a similar effect could be caused by surface tension forces, as recently discussed in detail in ref 82, the viscosity growth is absent for the pure solvent and for R50 copolymer in the same shear stress range, as is seen from Figure 8. So we think that the intrinsic viscosity anomaly and yield stress detected for MB50 are indicative of real structures existing in the multiblock VAc–VA copolymer solutions.

Semidilute and Concentrated Solutions. We started to study rheological properties of 5% solutions of R50 and MB52 VAc–VA copolymers in DMSO being aware of the nonhomogeneity of atactic PVA solutions,[83] which was related to the intermolecular H-bonding of VA units. It was found (see Figure S9 in the Supporting Information) that at a low shear stress both copolymers, as well as homopolymers PVA and PVAc, demonstrate solid-like behavior, which can be described by the simplest Kelvin–Voigt model with $G' = \text{const}$ and $G'' \sim \omega$. MB52 copolymer demonstrates the supramolecular structure similar to that of PVA, whereas the elasticity of R50 is even worse than in the case of PVAc, with considerably lower values of the storage modulus and the yield stress.

The presence of long VA blocks, which are able to multiple self-association through hydroxyl–hydroxyl H-bonds, appears to be the main factor that controls elasticity of the studied semidilute solutions. Unfortunately, the properties of DMSO solutions are rather unstable because of moisture uptake, which cannot be prevented during the rheology and light scatterilng experiments. Therefore, we made further experiments changing a solvent for DMF despite its worse dissolving ability for hydrogen-bonded substances.

5% solutions of VAc–VA copolymers in DMF behave practically as simple viscoelastic liquids, for which $G' \sim \omega^2$ and $G'' \sim \omega^1$ (Figure 9a). Note that the absolute values of the dynamic modulus components are considerably higher in the case of the multiblock copolymer. As discussed above, the random copolymer is characterized by a high amount of intrachain hydroxyl–acetyloxy H-bonds, whereas the multiblock copolymer possesses more "free" VA and VAc units that can interact through DMF molecules.

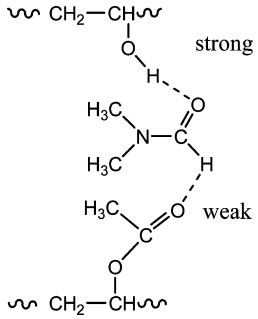

However, an H-bond between formyl (as well as methyl) hydrogen and carbonyl oxygen is very weak (2–3 kcal/mol)[84,85] and such interactions cannot give rise to a solid-like structure in the solutions. Indeed, there is no indication of a yield stress at the flow curves for 5% solutions of R50 and MB52 copolymers in Figure 10. As a result, elasticity of the studied solutions is governed by entanglements, whereas the chain structure has only a secondary effect. Note that for R50 copolymer at c = 10%, G' and G'' do not obey the above-mentioned regularities (Figure 9b), but still no yielding is observed (Figure 10).

The situation becomes completely different for MB52 at c = 10%. The corresponding flow curve in Figure 10 reveals already two vertical drops at σ = 0.1 and 0.6 Pa. The first one reflects destroying the solid-like structure of the solution described by nearly constant components of the dynamic modulus (Figure 9b). The second drop presumably corresponds to the shear-induced phase separation. The latter speculation is confirmed visually, since at high stresses jelly clots appear that can be easily separated from the solution. Thus, a structure for-

dx.doi.org/10.1021/ma5003326 | Macromolecules 2014, 47, 4790–4804

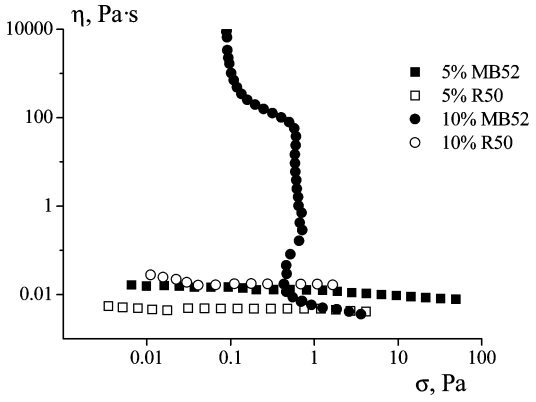

Figure 10. Flow curves in the rate-controlled mode for 5 and 10% solutions of R50 and MB52 in DMF at 20 °C.

mation in MB52 solution foreshadows phase separation at high stresses.

It is also necessary to notice that the shape of the flow curves presented in Figure 10 and some other figures below can lead to the stream instability and formation of shear bands. This phenomenon was reported for the various polymeric and colloid systems.[86−88] Though it was quite possible in our case, we did not study this effect.

A subtle distinction between 5% solutions of R50 and MB52 in DMF at 20 °C increases substantially upon cooling down the solutions to −20 °C (note that it is impossible for solutions in DMSO, which crystallizes at 18 °C). As is seen from Figure 11a, the spatial structure emerges in the both systems but its strength characterized by the yield stress differs by four orders of magnitude! It is clear that at low temperatures hydrogen bonds control the solution elasticity. We can speculate that worsening the solvent quality at cooling leads to a replacement of interchain H-bonds mediated by DMF molecules with hydroxyl-hydroxyl and hydroxyl-acetyloxy H-bonds formed directly between copolymer chains. As explained above, the multiblock VAc−VA copolymer is more capable of their formation than the random copolymer of a close composition but even in the latter case the dynamic viscosity considerably increases upon cooling.

It is worth mentioning that an abrupt change of the rheological characteristics recently reported for PAN solutions in DMSO and DMF upon heating[89] or adding water[90] was in the both cases also related to changing the prevailing type of specific interchain interactions.

MB83, R13, and R26 copolymers also demonstrate a weak non-Newtonian behavior at −20 °C, the structure formed by the multiblock copolymer with a high percentage of VAc units being only a bit stronger than those of the random copolymers with prevailing fraction of VA units (Figure 11b). R70 copolymer, as well as homopolymer PVAc solutions, does not reveal any unusual behavior at −20 °C, whereas MB15 and MB26 form jellies up to 90 °C, when the prevailing hydroxyl-hydroxyl H-bonds begin to dissociate, according to the IR data (see Table S1). Thus, the structure of VAc−VA copolymer chains appears to be as important as their composition, at least for the studied rheological properties.

Formation of a strong spatial structure can take a certain time thus resulting in the markedly slow kinetic transition for 5% MB52 solution, which is absent for R50 copolymer (Figure 12). At a given temperature below 60 °C, the viscosity of the former system at cooling and heating can be considerably different, up to the order of magnitude. Temperature width of the hysteresis loop measured between the steepest parts of the heating and cooling curves (marked by vertical dashes) equals 18 °C.

At high shear rates, when the spatial solid-like structure is destroyed, the viscosity is independent of the shear rate and can be treated as a measure of a solute size. Since the multiblock and random copolymers are of similar degrees of polymerization, a systematic difference in the specific viscosity, which is clearly visible in Figure 13, just means that MB copolymers preserve their tendency to aggregation at all compositions, as long as they are soluble. It is seen that the specific viscosity of MB copolymer solutions in DMF linearly increases with the fraction of VA units, whereas for R copolymer solutions it stays roughly constant until the equimolar composition is reached and begins to grow only for copolymers with the prevailing fraction of VA units.

Light Scattering. The time relaxation spectra of R50 and MB52 solutions in DMF, which were reconstructed from the correlation functions of scattered light measured in the DLS experiments, are shown in Figure 14 for the concentration range of 0.5−5%. The random copolymer behavior (left column) is typical for polymer solutions.[91] At the lowest tested concentration, c = 0.25%, there is a single relaxation mode due to the diffusion of isolated chains. Starting from c = 0.5%, two modes are observed, which means that an overlap concentration

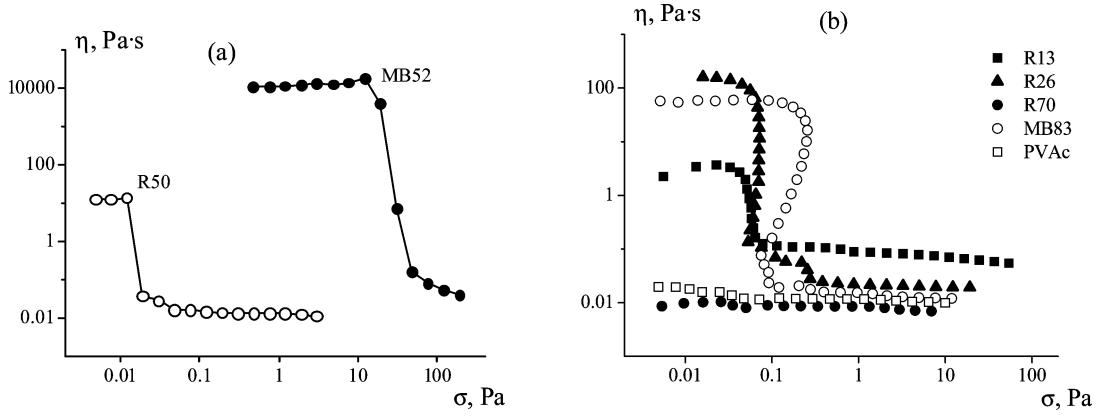

Figure 11. Flow curves for 5% solutions of (a, the stress-controlled mode) R50, MB52 copolymers and (b, the rate-controlled mode) R13, R26, R70, MB83 copolymers and PVAc in DMF at T = 20 °C.

dx.doi.org/10.1021/ma5003326 | Macromolecules 2014, 47, 4790−4804

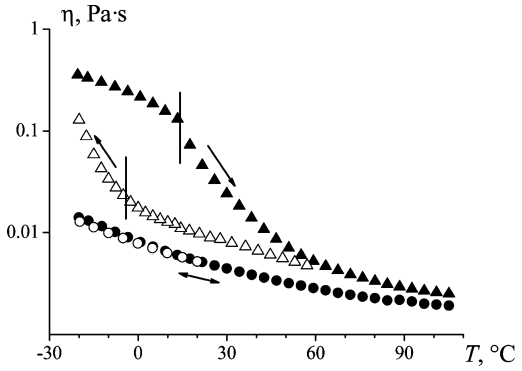

Figure 12. Temperature dependence of the apparent viscosity for the 5% solutions of R50 (circles) and MB52 (triangles) copolymers in DMF measured in the heating (5 °C/min) to cooling (1 °C/min) cycle at a fixed shear rate of 100 s^{-1}.

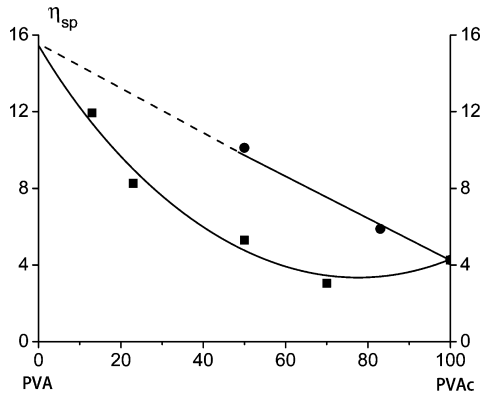

Figure 13. Specific viscosity of the 5% multiblock (circles) and random (squares) copolymer solutions in DMF measured at high shear rates.

separating the dilute and semidilute regimes is passed. A fast mode reflects the cooperative diffusion of chain segments, whereas a slow mode is system-dependent but always related to interchain interactions because it is absent up to the concentrated solutions only in good solvents.[92] For instance, the slow mode was detected for hydrophobically associating statistical copolymers of styrene and methyl methacrylate in a selective solvent (acetone).[93] In our case, this mode appears due to H-bonding, which promotes the formation of chain clusters that diffuse thus contributing to the relaxation of concentration fluctuations. Since the slow mode was also observed in the semidilute aqueous solutions of homopolymer PVA,[94−97] the interaction between VA units seems to play a major role in its genesis.

However, appearance of the slow mode is not accompanied by an abrupt growth in the total intensity of scattered light, which means that clustering due to H-bonding does not lead to a phase transition, but it is just a consequence of exceeding the overlap threshold. With further increasing concentration of R50 solution, the fast mode becomes faster and its contribution to the total relaxation decreases, while the slow mode gets slower but relatively more important, which is generally expectable.[91]

The relaxation spectrum of the multiblock copolymer solution (Figure 14, right column) contains a number of features. First, it is shifted to longer times by approximately an order of magnitude, which can be explained by higher viscosity of MB solutions (Figures 12 and 13), and it correlates with the considerably longer mechanical relaxation of MB copolymers in the bulk (Figure 6). At c = 0.5%, the spectrum is still unimodal, which means that the overlap concentration is higher than that for the random copolymer solution. Since chains overlap, when a polymer concentration in the solution becomes equal to that within the volume of one chain, we conclude that the conformation of MB52 chains in solution is more compact than that of R50 ones. In other words, DMF is a worse solvent for the multiblock copolymer, in accordance with the FTIR spectroscopy data that residual DMF volatilizes from it at a much lower temperature of 80 °C than from the random copolymer (150 °C). Moreover, it explains our problem with a low dissolution rate of MB52 mentioned in the Experimental Section.

Nevertheless, at $c \geq$ 1% DLS detects two relaxation modes and at c = 4.5% a third mode arises (in Figure 14, the spectrum for c = 5% is shown), which possesses an intermediate relaxation time and amplitude close to that of the fast mode. The origin of the intermediate mode is not clear.

The concentration behavior of the fast mode seems rather unusual, as its characteristic time increases, while the amplitude decreases, though very slowly. It is expected that fluctuations should relax by the cooperative diffusion faster in a more concentrated system, where the osmotic pressure is higher. However, the equilibrium number density of H-bonds hampering diffusive relaxation also grows with concentration. We can only speculate that the distribution of associating groups in macromolecules appears to be a decisive factor that governs the difference in the fast mode behavior for R50 and MB52 solutions.

Strong hydrogen bonding in the multiblock copolymer results in the formation of large chain clusters, as follows from the angular dependence of the scattered light intensity obtained from SLS experiments and plotted in Figure 15. Whereas the intensity is almost constant for R50, it considerably drops at high scattering angles for MB52. It means that MB52 solution contains objects larger than $2\pi/q$, the value of which varies between 525 and 229 nm for the studied angle range 50−150°. In this connection, it is indicative that it was impossible to filter MB52 solution through a Nylon membrane with the pore size of 450 nm.

By measuring the intensity at different scattering angles, one obtains the dependence of the mode average relaxation rate Γ_i on the wave vector q. At c = 5% all five modes, two in the case of the random copolymer and three belonging to the multiblock one, appear to be of diffusive nature (Figure 16). It corroborates the rheological finding (see Figure 9a) that 5% solutions of VAc−VA copolymers demonstrate the simple viscoelastic behavior at 20−25 °C. In other words, they are not gels. The slopes of the fitting straight lines in Figure 16 give the corresponding diffusion coefficients.

Assuming that the relaxation remains diffusive at smaller concentrations, we calculated and plotted in Figure 17 the concentration dependences of the diffusion coefficients. For the random copolymer (Figure 17a), the data are highly scattered because of the low intensity of light transmitted by the colored solution. The fast mode diffusivity D_f grows by an order of magnitude in the studied concentration range, though the scaling law cannot be fully concluded. The slow mode diffusivity at $c >$ 2% begins to decrease as $D_s \sim c^{-5/4}$ and this regime could be considered as a crossover to the scaling law $D_s \sim c^{-7/4}$ characterizing chain motion in the well-entangled regime. For the multiblock copolymer (Figure 17b), all three diffusivities decrease with the concentration. It is seen that the increased

dx.doi.org/10.1021/ma5003326 | Macromolecules 2014, 47, 4790−4804

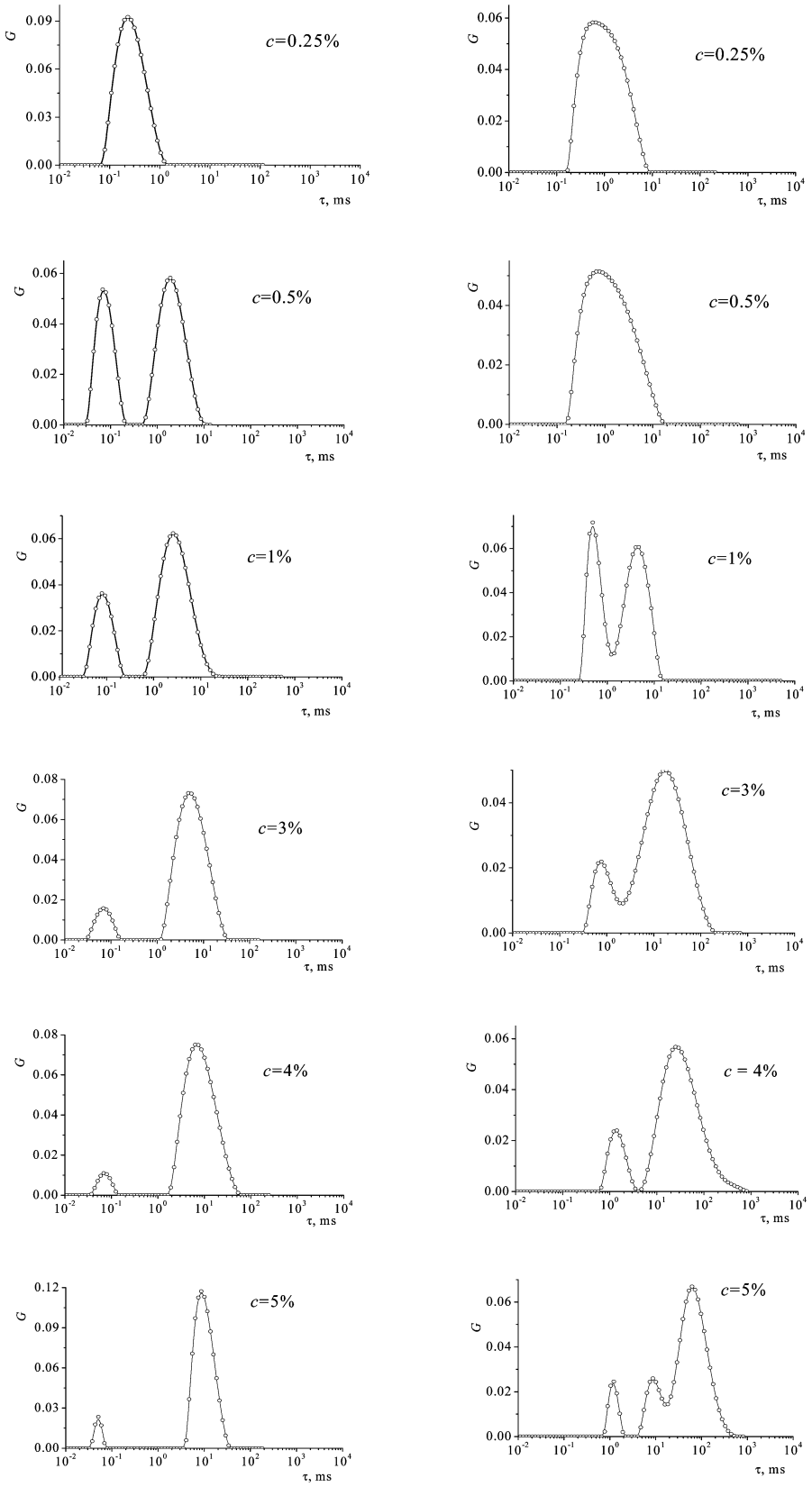

Figure 14. Concentration dependences of the characteristic relaxation time distributions of (left) R50 and (right) MB52 copolymer solutions in DMF measured by DLS at $\theta = 90°$ and 25 °C.

clustering due to hydrogen bonds hampers both of them (D_f is nearly independent of c and $D_s \sim c^{-2}$ at $c > 2\%$) in comparison to the scaling predictions and our data for R50 copolymer.

The hydrodynamic screening length can be found as $\xi_h = k_B T/(6\pi\eta_0 D_f)$, where η_0 is the pure DMF viscosity. At 25 °C, $\eta_0 = 0.802$ mPa·s so that in the dilute regime ($c = 0.25\%$), we

dx.doi.org/10.1021/ma5003326 | Macromolecules 2014, 47, 4790−4804

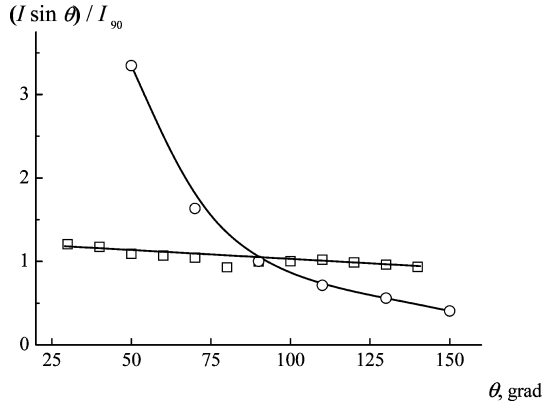

Figure 15. Angular dependences of the scattered light intensity (scaled by the intensity at $\theta = 90°$) for 5% solutions of R50 (squares) and MB52 (circles) copolymers in DMF at 25 °C.

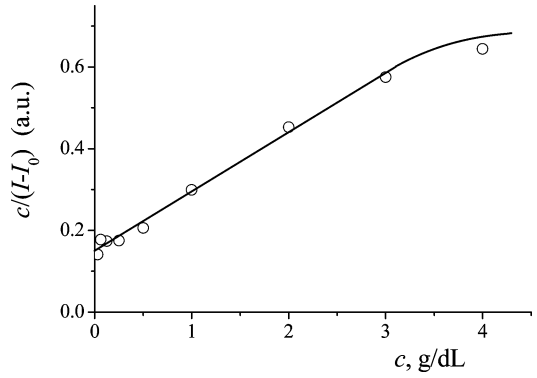

Figure 18. Concentration dependence of the concentration to the relative intensity ratio for MB52 copolymer solution in DMF at $\theta = 90°$ and 25 °C.

get ξ_h = 30 nm for R50 and 88 nm for MB52 solutions. The former value is a good estimate for the hydrodynamic radius R_h of a swollen macromolecule containing 450 monomer units, whereas the latter one is too much for a single chain of the same polymerization degree. Since $R_h \sim M^{\nu}$, a 3-fold increase in R_h should correspond to an aggregate of 6−7 chains in good solvent ($\nu = 0.6$). However, as we already know, DMF is not as good for MB52 as for R50 chains, so that multiblock macromolecules are more compact and an aggregate can contain of the order of 10 such chains.

Thus, we come to a conclusion that dilution does not break chain aggregates in the solution of MB52 in DMF, contrary to the diluted aqueous solutions of PVA, which contain only individual chains.[97] In order to check it, we conducted several additional SLS experiments by diluting MB52 solution down to the concentration of 0.031%. As is seen from Figure 18, the dependence of $c/(I - I_0)$ on c, where I is the total scattered

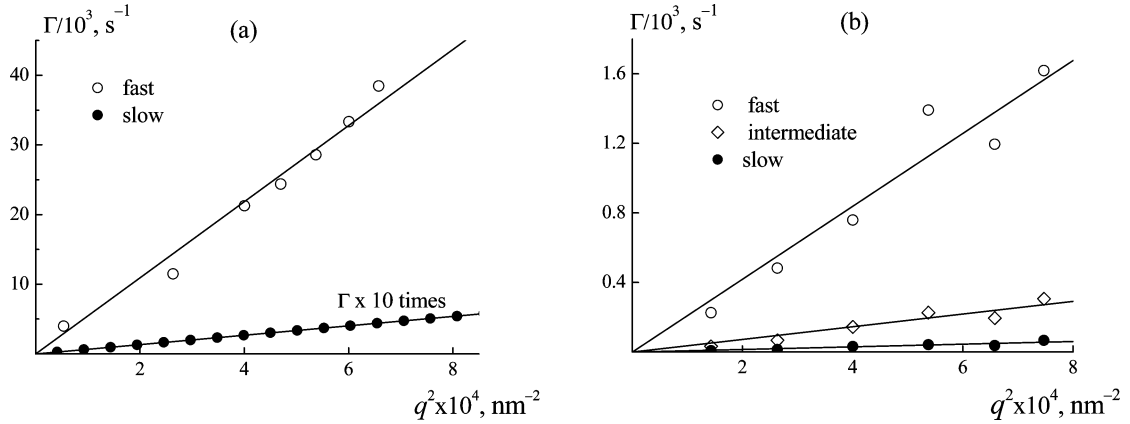

Figure 16. Average relaxation rates of the DLS modes for 5% solutions of (a) R50 and (b) MB52 copolymers in DMF at 25 °C vs squared scattering wave vector q^2.

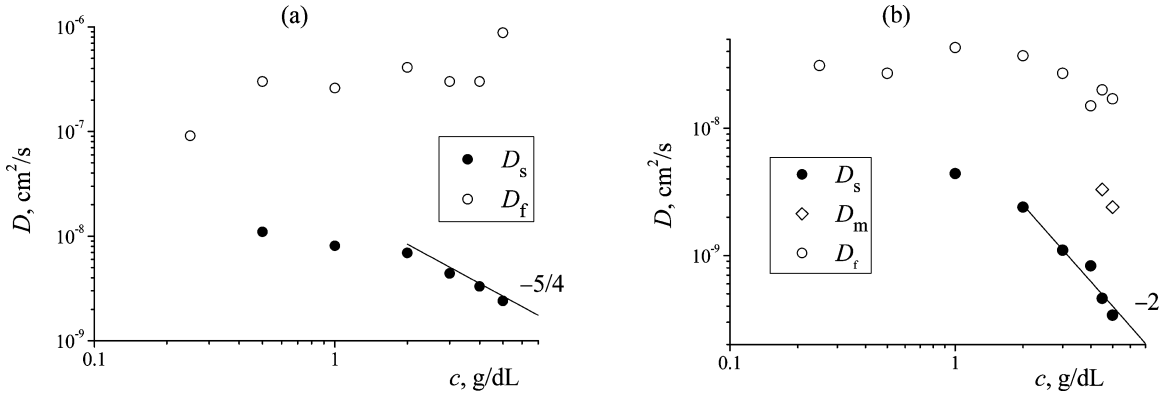

Figure 17. Concentration dependences of the diffusion coefficients characterizing the DLS relaxation modes (a) R50 and (b) MB52 copolymer solutions in DMF at 25 °C.

dx.doi.org/10.1021/ma5003326 | Macromolecules 2014, 47, 4790−4804

light intensity and I_0 is its pure solvent value, can be fitted by a straight line up to c = 3 g/dL, in accordance with the well-known Debye equation. Thus, we may conclude that no abrupt aggregation or disaggregation takes place.

Independence of an aggregate size on the concentration, which is proved by the LS experiments, is essential for explaining the reduced viscosity anomaly in MB52 dilute solutions (Figure 7). Those aggregates can be destroyed by a shear field in a rotational rheometer only if enough high stress is applied, as is seen from Figure 8.

CONCLUSIONS

Comparison of well-characterized random and multiblock copolymers of vinyl acetate and vinyl alcohol demonstrated essential differences in their rheological properties in dilute and semidilute solutions, as well as in the bulk state. Aside from the expectable effect of the copolymer composition, the strong influence of the comonomer unit distribution was detected for the first time. While the difference in the average block lengths for the mostly studied equimolar VAc–VA copolymers (ca. two monomer units in the random copolymer and five in the multiblock one) may seem subtle, it is responsible for many features in their dynamical behavior caused by hydrogen bond interactions.

Even rather short blocks of identical monomer units in a multiblock macromolecule retain their own relaxation properties and prevent creating a common spectrum for the whole chain. This puts some limits on the applicability of the frequency–temperature superposition. The superposition fails progressively when applied to the multiblock copolymers with a growing fraction of crystallizable vinyl alcohol monomer units, since partial crystallization excludes the terminal zone.

Numerous features are found in the solution behavior of the random and multiblock VAc–VA copolymers. The main differences are related to the yielding due to the self-assembling of blocks, which results in the solid-like behavior at low stresses. This structure is kept even in dilute solutions and it manifests itself at higher concentrations by a large yield stress and the dynamic viscosity–temperature hysteresis behavior that are observed in the copolymers containing longer VA blocks. Cooling the solution results in replacing the solvent-mediated H-bonds with the direct interchain ones that tremendously strengthen the solid-like structure.

At the same time, DLS does not reveal any gel modes so that concentration fluctuations relax via two diffusive processes in the random copolymers and three in the multiblock ones. In the latter case, the fast mode does not get faster with increasing concentration, which could be related to the presence of H-bonds.

According to the IR data, the multiblock copolymers are characterized by stronger hydroxyl-hydroxyl H-bonds up to 210 °C, while the random copolymers more strongly interact with residual DMF solvent and contain its traces up to 150 °C. Hydroxyl-acetyloxy H-bonds also persist up to high temperatures. Such intrachain bonds are readily formed between neighboring VAc and VA units, which are more numerous in the random copolymers. On the contrary, interchain hydroxyl-acetyloxy H-bonds are more typical for the multiblock copolymers thus strengthening their tendency to association.

Concentrated multiblock copolymer solutions are characterized by a two-step yielding that indicates the possibility of a shear-induced phase separation at high stresses, which follows the destruction of the weak solid-like structure.

Since we believe that the difference between multiblock and random VAc–VA copolymers behavior stems from H-bonding, it is instructive to draw a scheme that summarizes our considerations:

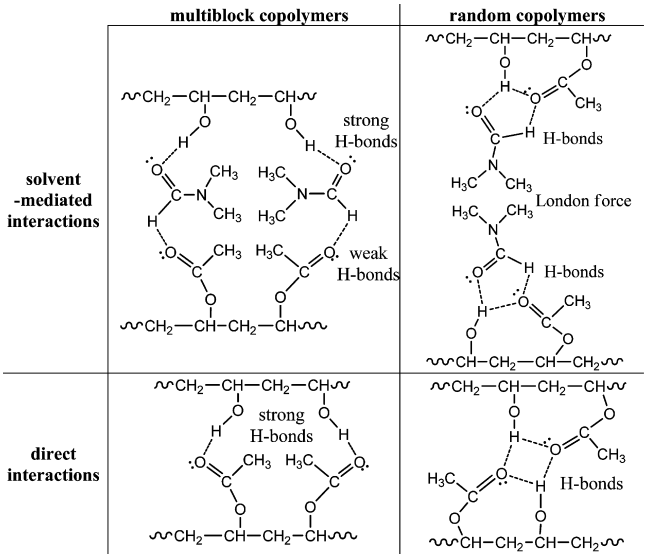

Though only hydroxyl-acetyloxy H-bonds are depicted, the main idea is clear: many neighboring VA and VAc units in the random copolymer form intrachain H-bonds thus hindering interchain interactions, which appear to be considerably stronger in the multiblock copolymer. At lower temperatures, when the solvent is poorer, or in the bulk, this difference is even more pronounced as copolymer chains interact directly. Thus, our results demonstrate that the chain structure of statistical copolymers can be at least as important as their composition in determining their tendency to self-assembling, which can be revealed through studying various structure-properties relations.

ASSOCIATED CONTENT

Supporting Information

NMR and FTIR spectra, DSC traces in comparison to the temperature dependences of the dynamic modulus, and frequency dependences of the storage and loss moduli for the random and multiblock vinyl acetate–vinyl alcohol copolymers at different temperatures, and rheological properties of semidilute solutions of those copolymers in DMSO. This material is available free of charge via the Internet at http://pubs.acs.org

AUTHOR INFORMATION

Corresponding Author

*(Y.V.K.) E-mail: yar@ips.ac.ru.

Notes

The authors declare no competing financial interest.

ACKNOWLEDGMENTS

The authors are thankful to A. S. Peregudov (Nesmeyanov Institute of Organoelement Compounds RAS) for performing NMR measurements. The work was partially supported by the Russian Foundation for Basic Research (Project 13-03-00016).

REFERENCES

(1) Badi, N.; Chan-Seng, D.; Lutz, J.-F. *Macromol. Chem. Phys.* **2013**, *214*, 135–142.
(2) Abetz, V.; Simon, P. F. W. *Adv. Polym. Sci.* **2005**, *189*, 125–212.

(3) Bates, F. S.; Hillmyer, M. A.; Lodge, T. P.; Bates, C. M.; Delaney, K. T.; Fredrickson, G. H. *Science* **2012**, *336*, 434−440.
(4) Hamley, I. W. *Prog. Polym. Sci.* **2009**, *34*, 1161−1210.
(5) Kim, H.-C.; Park, S.-M.; Hinsberg, W. D. *Chem. Rev.* **2010**, *110*, 146−177.
(6) Zhang, H.; Shen, P. K. *Chem. Rev.* **2012**, *112*, 2780−2832.
(7) Genzer, J.; Khalatur, P. G.; Khokhlov, A. R. In *Polymer Science: A Comprehensive Reference*; Matyjaszewski, K., Möller, M., Eds.; Elsevier BV: Amsterdam, 2012; Vol. *6*, pp 689−723.
(8) Liu, R.; Fraylich, M.; Saunders, B. R. *Colloid Polym. Sci.* **2009**, *287*, 627−643.
(9) Lutz, J.-F. *Adv. Mater.* **2011**, *23*, 2237−2243.
(10) Galvin, C. J.; Genzer, J. *Prog. Polym. Sci.* **2012**, *37*, 871−906.
(11) Shakhnovich, E. I.; Gutin, A. M. *J. Phys. (Fr.)* **1989**, *50*, 1843−1850.
(12) Fredrickson, G. H.; Milner, S. T.; Leibler, L. *Macromolecules* **1992**, *25*, 6341−6354.
(13) Angerman, H.; ten Brinke, G.; Erukhimovich, I. *Macromolecules* **1996**, *29*, 3255−3262.
(14) Subbotin, A. V.; Semenov, A. N. *Eur. Phys. J. E* **2002**, *7*, 49−64.
(15) Kuchanov, S. I.; Panyukov, S. V. *J. Phys.: Condens. Matter* **2006**, *18*, L43−L48.
(16) von der Heydt, A.; Müller, M.; Zippelius, A. *Phys. Rev. E* **2011**, *83*, 051131.
(17) Swift, B. W.; Olvera de la Cruz, M. *Europhys. Lett.* **1996**, *35*, 487−492.
(18) Litmanovich, A. D.; Kudryavtsev, Y. V.; Kriksin, Y. A.; Kononenko, O. A. *Macromol. Theory Simul.* **2003**, *12*, 11−16.
(19) Houdayer, J.; Müller, M. *Macromolecules* **2004**, *37*, 4283−4295.
(20) Litmanovich, A. D.; Podbelskiy, V. V.; Kudryavtsev, Y. V. *Macromol. Theory Simul.* **2010**, *19*, 269−277.
(21) Gavrilov, A. A.; Kudryavtsev, Y. V.; Khalatur, P. G.; Chertovich, A. V. *Chem. Phys. Lett.* **2011**, *503*, 277−282.
(22) Gavrilov, A. A.; Kudryavtsev, Y. V.; Chertovich, A. V. *J. Chem. Phys.* **2013**, *139*, 224901.
(23) Steinmüller, B.; Müller, M.; Hambrecht, K. R.; Smith, G. D.; Bedrov, D. *Macromolecules* **2012**, *45*, 1107−1117.
(24) Steinmüller, B.; Müller, M.; Hambrecht, K. R.; Bedrov, D. *Macromolecules* **2012**, *45*, 9841−9853.
(25) Slimani, M. Z.; Moreno, A. J.; Rossi, G.; Colmenero, J. *Macromolecules* **2013**, *46*, 5066−5079.
(26) Gao, H.; Vadlamudi, M.; Alamo, R. D.; Hu, W. *Macromolecules* **2013**, *46*, 6498−6506.
(27) Park, H. E.; Dealy, J. M.; Marchand, G. R.; Wang, J.; Li, S.; Register, R. A. *Macromolecules* **2010**, *43*, 6789−6799.
(28) Reid, O. B.; Vadlamudi, M.; Mamun, A.; Janani, H.; Gao, H.; Hu, W.; Alamo, R. D. *Macromolecules* **2013**, *46*, 6485−6497.
(29) Ratna, D.; Karger-Kocsis, J. *J. Mater. Sci.* **2008**, *43*, 254−269.
(30) Norris, B. N.; Zhang, S.; Campbell, C. M.; Auletta, J. T.; Calvo-Marzal, P.; Hutchinson, G. R.; Meyer, T. Y. *Macromolecules* **2013**, *46*, 1384−1392.
(31) Park, C. H.; Lee, C. H.; Guiver, M. D.; Lee, Y. M. *Prog. Polym. Sci.* **2011**, *36*, 1443−1498.
(32) Leibler, L. *Prog. Polym. Sci.* **2005**, *30*, 898−914.
(33) Fredrickson, G. H. *The Equilibrium Theory of Inhomogeneous Polymers*; Oxford University Press: New York, 2006.
(34) Lynd, N. A.; Meuler, A. J.; Hillmyer, M. A. *Prog. Polym. Sci.* **2008**, *33*, 875−893.
(35) Meuler, A. J.; Ellison, C. J.; Qin, J.; Evans, C. M.; Hillmyer, M. A.; Bates, F. S. *J. Chem. Phys.* **2009**, *130*, 234903.
(36) Li, S.; Register, R. A.; Landes, B. G.; Hustad, P. D.; Weinhold, J. D. *Macromolecules* **2010**, *43*, 4761−4770.
(37) Wang, Y.; Li, X.; Tang, P.; Yang, Y. *Physica B* **2011**, *406*, 1132−1138.
(38) Widin, J. M.; Schmitt, A. K.; Scmitt, A. L.; Im, K.; Mahanthappa, M. K. *J. Am. Chem. Soc.* **2012**, *134*, 3834−3844.
(39) Li, Y.; Qian, H.-J.; Lu, Z.-Y. *Polymer* **2013**, *54*, 3716−3722.
(40) Brown, J. R.; Sides, S. W.; Hall, L. M. *ACS Macro Lett.* **2013**, *2*, 1105−1109.
(41) Pandav, G.; Ganesan, V. *J. Chem. Phys.* **2013**, *139*, 214905.
(42) Pandav, G.; Ganesan, V. *Macromolecules* **2013**, *46*, 8334−8344.
(43) Chum, P. S.; Swogger, K. W. *Prog. Polym. Sci.* **2008**, *33*, 797−819.
(44) Badi, N.; Lutz, J.-F. *Chem. Soc. Rev.* **2009**, *38*, 3383−3390.
(45) Rosales, A. M.; Segalman, R. A.; Zuckermann, R. N. *Soft Matter* **2013**, *9*, 8400−8414.
(46) Platé, N. A.; Litmanovich, A. D.; Noah, O. V. *Macromolecular Reactions. Peculiarities, Theory, and Experimental Approaches*; Wiley: New York, 1995.
(47) Ahmed, I.; Pritchard, J. G. *Polymer* **1979**, *20*, 1492−1496.
(48) Joshi, D. P.; Pritchard, J. G. *Polymer* **1978**, *19*, 427−430.
(49) Tubbs, R. K. *J. Polym. Sci., Part A-1* **1966**, *4*, 623−629.
(50) Helfand, M. A.; Mazzanti, J. B.; Fone, M.; Reamey, R. H.; Lindley, P. M. *Langmuir* **1996**, *12*, 1296−1302.
(51) Moritani, T.; Fujiwara, Y. *Macromolecules* **1977**, *10*, 532−535.
(52) Sakurada, I. *Pure Appl. Chem.* **1968**, *16*, 263−284.
(53) Arranz, F.; Ashraf-Tahir, M. *Rev. Plast. Mod.* **1969**, *20*, 777−781.
(54) Turska, E.; Jantas, R. *J. Polym. Sci., Polym. Symp.* **1974**, *47*, 359−368.
(55) Garnaik, B.; Thombre, S. M. *J. Appl. Polym. Sci.* **1999**, *72*, 123−133.
(56) Isasi, J. R.; Cesteros, L. C.; Katime, I. *Macromolecules* **1994**, *27*, 2200−2205.
(57) Finch, C. A., Ed. *Polyvinyl Alcohol*; Wiley: New York, 1973.
(58) Denisova, Yu. I.; Krentsel', L. B.; Peregudov, A. S.; Litmanovich, E. A.; Podbel'skiy, V. V.; Litmanovich, A. D.; Kudryavtsev, Y. V. *Polym. Sci. Ser. B* **2012**, *54*, 375−382.
(59) Denisova, Yu. I.; Shandryuk, G. A.; Krentsel', L. B.; Blagodatskikh, I. V.; Peregudov, A. S.; Litmanovich, A. D.; Kudryavtsev, Y. V. *Polym. Sci. Ser. A* **2013**, *55*, 385−392.
(60) Müller, A. J.; Arnal, M. L. *Prog. Polym. Sci.* **2005**, *30*, 559−603.
(61) Tamura, E.; Kawai, Y.; Inoue, T.; Watanabe, H. *Macromolecules* **2012**, *45*, 6580−6586.
(62) Tan, H.; Watanabe, H.; Matsumiya, Y.; Kanaya, T.; Takahashi, Y. *Macromolecules* **2003**, *36*, 2886−2893.
(63) Matsumiya, Y.; Watanabe, H.; Takano, A.; Takahashi, Y. *Macromolecules* **2013**, *46*, 2681−2695.
(64) Uneyama, T.; Suzuki, S.; Watanabe, H. *Phys. Rev. E* **2012**, *86*, 031802.
(65) Suzuki, S.; Uneyama, T.; Inoue, T.; Watanabe, H. *Macromolecules* **2012**, *45*, 888−898.
(66) Van der Velden, G.; Beulen, J. *Macromolecules* **1982**, *15*, 1071−1075.
(67) Dutta, K.; Mukherjee, M.; Brar, A. S. *J. Polym. Sci., Part A: Polym. Chem.* **1999**, *37*, 551−556.
(68) Bellami, L. J. *The Infrared Spectra of Complex Molecules*; Champan & Hall: London, 1980; Vol. 2.
(69) Fesko, D. G.; Tschoegl, N. W. *J. Polym. Sci., Part C* **1971**, *35*, 51−69.
(70) Hodge, I. M. *J. Non-Cryst. Solids* **1994**, *169*, 211−266.
(71) Tubbs, R. K. *J. Polym. Sci., Part A: Polym. Chem.* **1965**, *3*, 4181−4189.
(72) Flory, P. J. *Trans. Faraday Soc.* **1955**, *51*, 848−857.
(73) Kossuth, M. B.; Morse, D. C.; Bates, F. S. *J. Rheol.* **1999**, *43*, 167−196.
(74) Kawasaki, K.; Onuki, A. *Phys. Rev. A* **1990**, *42*, 3664−3666.
(75) Watanabe, H. Rheology of Multiphase Polymeric Systems. In *Structure and Properties of Multiphase Polymeric Materials*; Araki, T., Qui, T. C., Shibayama, M., Eds.; Marcel Dekker: New York, 1998; Chapter 9.
(76) He, P.; Shen, W.; Yu, W.; Zhou, C. *Macromolecules* **2014**, *47*, 807−820.
(77) Reilly, P. M.; van der Hoff, B. M. E.; Ziogas, M. *J. Appl. Polym. Sci.* **1979**, *24*, 2087−2100.
(78) Staudinger, H. *Die hochmolekularen organischen Verbindungen*; Springer: Berlin, 1932; p 201.
(79) Brunchi, C.-E.; Bercea, M.; Morariu, S. *High Perform. Polym.* **2008**, *20*, 311−322.

(80) Malkin, A.; Ilyin, S.; Roumyantseva, T.; Kulichikhin, V. *Macromolecules* **2013**, *46*, 257−266.
(81) Ilyin, S.; Roumyantseva, T.; Spiridonova, V.; Semakov, A.; Frenkin, E.; Malkin, A.; Kulichikhin, V. *Soft Matter* **2011**, *7*, 9090−9103.
(82) Johnson, M. T.; Ewoldt, R. H. *J. Rheol.* **2013**, *57*, 1515−1532.
(83) Lee, E. J.; Kim, N. H.; Dan, K. S.; Kim, B. C. *J. Polym. Sci., Part B: Polym. Phys.* **2004**, *42*, 1451−1456.
(84) Park, S.-K.; Min, K.-C.; Lee, C.; Hong, S. K.; Kim, Y.; Lee, N.-S. *Bull. Korean Chem. Soc.* **2009**, *30*, 2595−2602.
(85) Zhang, C.; Ren, Z.; Liu, L.; Yin, Z. *Mol. Simul.* **2013**, *39*, 875−881.
(86) Møller, P. C. F.; Rodts, S.; Michels, M. A. J.; Bonn, D. *Phys. Rev. E* **2008**, *77*, 041507.
(87) Malkin, A.; Ilyin, S.; Semakov, A.; Kulichikhin, V. *Soft Matter* **2012**, *8*, 2607−2617.
(88) Ovarlez, G.; Rodts, S.; Chateau, X.; Coussot, P. *Rheol. Acta* **2009**, *48*, 831−844.
(89) Eom, Y.; Kim, B. C. *Polymer* **2014**, *55*, 2570−2577.
(90) Ilyin, S. O.; Kulichikhin, V. G.; Malkin, A. Ya. *Polym. Sci. Ser. A* **2013**, *55*, 503−509.
(91) Li, J.; Ngai, T.; Wu, C. *Polym. J.* **2010**, *42*, 609−625.
(92) Brown, N.; Nicolai, T. *Colloid Polym. Sci.* **1990**, *268*, 977−990.
(93) Konak, C.; Helmstedt, M.; Bansil, R. *Macromolecules* **1997**, *30*, 4342−4346.
(94) Horkay, F.; Burchard, W.; Geissler, E.; Hecht, A.-M. *Macromolecules* **1993**, *26*, 1296−1303.
(95) Kjøniksen, A.-L.; Nyström, B. *Macromolecules* **1996**, *29*, 7116−7123.
(96) Narita, T.; Knaebel, A.; Munch, J.-P.; Candau, S. J. *Macromolecules* **2001**, *34*, 8224−8231.
(97) Narita, T.; Mayumi, K.; Ducouret, G.; Hebraud, P. *Macromolecules* **2013**, *46*, 4174−4183.